Quantum Fisher information of the Greenberger-Horne-Zeilinger state in decoherence channels

Jian Ma,[1] Yi-xiao Huang,[1] Xiaoguang Wang,[1,*] and C. P. Sun[2]

[1]*Zhejiang Institute of Modern Physics, Department of Physics, Zhejiang University, Hangzhou 310027, China*

[2]*Institute of Theoretical Physics, Chinese Academy of Sciences, Beijing 100190, China*

(Received 29 March 2011; published 2 August 2011; corrected 28 September 2011)

Quantum Fisher information of a parameter characterizes the sensitivity of the state with respect to changes of the parameter. In this article, we study the quantum Fisher information of a state with respect to SU(2) rotations under three decoherence channels: the amplitude-damping, phase-damping, and depolarizing channels. The initial state is chosen to be a Greenberger-Horne-Zeilinger state of which the phase sensitivity can achieve the Heisenberg limit. By using the Kraus operator representation, the quantum Fisher information is obtained analytically. We observe the decay and sudden change of the quantum Fisher information in all three channels.

DOI: 10.1103/PhysRevA.84.022302 PACS number(s): 03.67.−a, 03.65.Ud, 03.65.Yz

I. INTRODUCTION

Fisher information plays a central role in estimation theory [1,2]. It quantifies the information that we can extract about a parameter from a probability distribution [e.g., $P(x|\theta)$ characterized by a parameter θ, with x the random variable]. A larger Fisher information means that we can estimate the parameter with a higher precision. Quantum Fisher information (QFI) [1–4] is the extension of Fisher information in a quantum regime, and the extension is natural since the description of quantum mechanics is essentially probabilistic. It is related to Ulhmann's fidelity [5–8] and is proportional to the Bures metric [4,9,10], which is the metric of the state space. Moreover, QFI characterizes the sensitivity of a state with respect to the perturbation of the parameter. The parameter to be estimated is usually associated with the frequency of the system, the phase difference gained during the evolution, and the strength of an external field. How to improve the precision of parameter estimation has been the focus of research for many years [11], and is of important applications in quantum technology like quantum frequency standards [12], measurement of gravity accelerations [13], clock synchronization [14], and so on.

So far, we know that entangled states are useful resources to improve the precision of parameter estimation [11,15–29] since entangled states are generally more sensitive than separable states. The best estimation with separable states is bounded by the shot-noise limit, also called the standard quantum limit, proportional to $1/\sqrt{N}$, where N is the particle number. This precision can be improved to $1/N$ (i.e., the Heisenberg limit) when we use a maximally entangled state. However, as a tradeoff, since entangled states are usually more sensitive to the change of the external field, they are also sensitive to noise, thus are fragile in the presence of decoherence [30–45]. As discussed in Ref. [30], the precision in phase estimation with maximally entangled states reduces to that with the separable states in the presence of Markovian dephasing, while a recent study [44] showed that for non-Markovian dephasing, the phase sensitivity of the maximal entangled state can also beat the coherent spin state. In general, in the presence of decoherence, the Heisenberg level estimation cannot be achieved, and the ultimate precision limit in noisy metrology was obtained recently [45], in terms of the Kraus operators of the decoherence channels and the initial state.

In this article, we study the QFI of the Greenberger-Horne-Zeilinger (GHZ) state, which is a maximally entangled state, in the presence of decoherence. We use three decoherence channels instead of specified physical models. The channels are the amplitude-damping channel (ADC), phase-damping channel (PDC), and depolarizing channel (DPC). Although the channels seems to be toys as compared with concrete physical models, they indeed capture the essential physics of decoherence [5,6].

In the absence of decoherence, the phase sensitivity of the GHZ state attains the Heisenberg limit (i.e., the error of the phase estimation scales as $1/N$). In the presence of decoherence, its phase sensitivity reduces due to the loss of entanglement. The phase sensitivity refers to the sensitivity of the state with respect to SU(2) rotations, and is characterized by the maximal mean QFI, which is explained in Sec. II.

In this article, we obtain analytical expressions for maximal mean QFI in terms of decoherence strength p. Based on these expressions, two remarkable results are found. (a) Sudden changes of the maximal QFI are observed in all three channels, and this sudden-change feature is similar to that in entanglement [46–48] and spin squeezing [49]. (b) For the ADC, after the sudden-changing point, the maximal mean QFI returns back to the shot-noise level with the increase of the decoherence strength. For the PDC, the maximal QFI decays to the shot-noise level and remains unchanged in this level with the increase of p. For the DPC, the QFI decays with the increase of p, and at $p = 1$ the states becomes a fully mixed state, which is invariant with SU(2) rotations, and the maximal mean QFI becomes zero.

This paper is organized as follows. In Sec. II, we discuss the QFI and introduce the maximal mean QFI. Then in Sec. III, we present the decoherence channels and their Kraus operator representations. Afterward, in Sec. IV, the maximal mean QFI of the GHZ states in these decoherence channels are studied, and analytical results are obtained. Finally, a summary is provided in Sec. V.

*xgwang@zimp.zju.edu.cn

II. QUANTUM FISHER INFORMATION

In this section, we discuss the QFI and the maximal mean QFI. First, we take the Ramsey spectroscopy as an example. In the Ramsey spectroscopy, we estimate the phase difference ϕ between the ground and excited states gained during the free evolution. This phase difference ϕ is related to a physical observable $\hat{O}_\phi$, which measures the population difference between the ground and excited states. The precision of the parameter ϕ we can achieve is determined by the fluctuation of the observable $\hat{O}_\phi$, and the variance of the parameter ϕ is obtained by using the error propagation relation $\Delta\phi = \Delta\hat{O}_\phi/|\sqrt{\mathcal{N}_m}\partial\langle\hat{O}_\phi\rangle/\partial\phi|$, where $\mathcal{N}_m$ is the number of experiments.

Generally, consider a density matrix $\rho(\phi)$, with a parameter ϕ, the variance of the estimation of the parameter ϕ is limited by the quantum Cramér-Rao bound [1,2]

$$\Delta\hat{\phi} \geqslant \Delta\phi_{\mathrm{QCB}} \equiv \frac{1}{\sqrt{\mathcal{N}_m F}}, \tag{1}$$

where $\hat{\phi}$ is an unbiased estimator (i.e., $\langle\hat{\phi}\rangle = \phi$). Indeed, $\hat{\phi}$ is a map from the experimental data to the parameter space, and

$$F = \mathrm{tr}[\rho(\phi)L_\phi^2], \tag{2}$$

is the QFI for ϕ derived in Refs. [1,2], with L_ϕ the so-called symmetric logarithmic derivative determined by the following equation

$$\frac{\partial}{\partial\phi}\rho(\phi) = \frac{1}{2}[\rho(\phi)L_\phi + L_\phi\rho(\phi)]. \tag{3}$$

The Cramér-Rao bound gives the ultimate limit for the precision of ϕ that can be achieved.

Now we consider that the parameter ϕ is acquired by an SU(2) rotation

$$\rho_\phi = U_\phi\rho U_\phi^\dagger, \tag{4}$$

where $U_\phi = \exp(i\phi J_{\vec{n}})$ with

$$J_{\vec{n}} = \vec{J}\vec{n} = \sum_{\alpha=x,y,z}\frac{1}{2}n_\alpha\sigma_\alpha, \tag{5}$$

the angular momentum operator in the $\vec{n}$ direction, and σ_α are the Pauli matrices. With Eq. (3), we derive the explicit form of L_ϕ, and then we take it into Eq. (2) to obtain

$$F(\rho, J_{\vec{n}}) = \sum_{i\neq j}\frac{2(p_i - p_j)^2}{p_i + p_j}|\langle i|J_{\vec{n}}|j\rangle|^2 = \vec{n}\,\mathbf{C}\,\vec{n}^T, \tag{6}$$

where p_i and $|j\rangle$ are the eigenvalue and eigenvector of ρ, respectively, and $\vec{n}$ is a normalized three-dimensional vector. The matrix elements of the symmetric matrix $\mathbf{C}$ are given as

$$\mathbf{C}_{kl} = \sum_{i\neq j}\frac{(p_i - p_j)^2}{p_i + p_j}[\langle i|J_k|j\rangle\langle j|J_l|i\rangle + \langle i|J_l|j\rangle\langle j|J_k|i\rangle]. \tag{7}$$

The QFI $F(\rho, J_{\vec{n}})$ is the sensitivity of the state ρ with respect to rotations along the $\vec{n}$ direction. If ρ is a pure state, the above matrix can be simplified as

$$\mathbf{C}_{kl} = 2\langle J_k J_l + J_l J_k\rangle - 4\langle J_k\rangle\langle J_l\rangle, \tag{8}$$

and the QFI can be expressed as $F(\rho, J_{\vec{n}}) = 4(\Delta J_{\vec{n}})^2$ [4].

The above QFI $F(\rho, J_{\vec{n}})$ is $\vec{n}$ dependent. Below we shall study the maximal mean QFI [29]

$$\bar{F}_{\max} = \frac{1}{N}\max_{\vec{n}}F(\rho, J_{\vec{n}}) = \frac{\lambda_{\max}}{N}, \tag{9}$$

which is proved in the Appendix, where N is the number of two-level particles, $\lambda_{\max}$ is the largest eigenvalue of the symmetric matrix $\mathbf{C}$ (7). From the Cramér-Rao bound given in Eq. (1), if $\bar{F}_{\max} > 1$ we have $\Delta\phi_{\mathrm{QCB}} < \Delta\phi_{\mathrm{SN}} = 1/\sqrt{N}$ ($\mathcal{N}_m = 1$), where $\Delta\phi_{\mathrm{SN}}$ denotes the shot-noise level. Furthermore, $\bar{F}_{\max} > 1$ is a sufficient condition for entanglement [28], and for coherent spin state $\bar{F}_{\max} = 1$.

Below, we study the maximal mean QFI for the GHZ state under decoherence. Consider an N-qubit GHZ state

$$|\psi\rangle = \frac{1}{\sqrt{2}}(|0\rangle^{\otimes N} + |1\rangle^{\otimes N}), \tag{10}$$

by using Eq. (7), the maximal mean QFI for GHZ state can be computed as

$$\bar{F}_{\max} = \frac{\mathbf{C}_{zz}}{N} = \frac{4(\Delta J_z)^2}{N} = N, \tag{11}$$

thus the phase sensitivity is $\Delta\phi = 1/N$, which attains the Heisenberg limit.

III. DECOHERENCE CHANNELS

In this section, we present the definitions of the three decoherence channels (ADC, PDC, and DPC), as well as their significance in physics. In general, the decoherence channels are given in the Kraus representation

$$\mathcal{E}(\rho) = \sum_\mu E_\mu\rho E_\mu^\dagger, \tag{12}$$

where E_μ are the Kraus operators that satisfy

$$\sum_\mu E_\mu^\dagger E_\mu = \mathbb{1}, \tag{13}$$

where $\mathbb{1}$ is an identity matrix. The decoherence channels have simple forms to deal with, and lead to theoretical predictions being often in good agreement with experiments [5,6]. Below, we discuss the three channels separately.

A. Amplitude-damping channel

The ADC describes the dissipation process. For a single qubit, the Kraus operators of the ADC are

$$E_0 = \sqrt{s}|0\rangle\langle 0| + |1\rangle\langle 1|, \quad E_1 = \sqrt{p}|1\rangle\langle 0|, \tag{14}$$

where the decoherence strength $p = 1 - s$, represents the probability of decay from the upper level $|0\rangle$ to the lower level $|1\rangle$, with $s = \exp(-\gamma_1 t/2)$, and γ_1 is the damping rate.

The ADC is a prototype model for discussing dissipation interactions, and is related to the relaxation time $T_1 = 1/\gamma_1$ in the spin resonance or superconducting qubit [6]. The dissipation process described by the ADC can be found in the spontaneous emission of a two-level atoms at zero temperature in the Born-Markov approximation.

An illustrative way to understand decoherence channels is to employ the Bloch sphere. For ADC, the Bloch sphere is squeezed into an ellipsoid and shifts it toward the north pole. The radius in the x-y plane is reduced by a factor $\sqrt{s}$, while in the z direction it is reduced by a factor s.

B. Phase-damping channel

The Kraus operators for the PDC are given by

$$E_0 = \sqrt{s}\mathbb{1}, \quad E_1 = \sqrt{p}|0\rangle\langle 0|, \quad E_2 = \sqrt{p}|1\rangle\langle 1|. \tag{15}$$

The PDC is a prototype model of dephasing or pure decoherence (i.e., loss of coherence of a two-level state without any loss of the system's energy). The decoherence strength is comparable with a concrete dephasing model by replacing p with $1 - \exp(-\gamma_2 t/2)$, where γ_2 is associated with the $T_2 = 1/\gamma_2$ relaxation in spin resonance, and is the major obstacle in superconducting qubit based quantum computation. In experiments with trapped ions, the motional PDC can be implemented just by modulating the trap frequency, which changes the phase of the harmonic motion of ions [50,51].

As a result of the action of the PDC, the Bloch sphere is compressed by a factor $(1 - 2p)$ in the x-y plane. In Ref. [30], the entanglement-assisted metrology was studied with a dephasing model, which can be described by the PDC.

C. Depolarizing channel

The Kraus operators of the DPC are given by

$$\begin{aligned} E_0 &= \sqrt{1-p'}\,\mathbb{1}, \quad E_1 = \sqrt{\frac{p'}{3}}\sigma_x, \\ E_2 &= \sqrt{\frac{p'}{3}}\,\sigma_y, \quad E_3 = \sqrt{\frac{p'}{3}}\sigma_z, \end{aligned} \tag{16}$$

where $p' = 3p/4$. For the DPC, the spin is depolarized to the maximally mixed state $\mathbb{1}/2$ with probability p or is unchanged with probability $s = 1 - p$, thus the radius of the Bloch sphere is reduced by a factor s, but its shape remains unchanged. The parameter estimation of the DPC was discussed in Ref. [32]

The above three channels covers considerable types of decoherence in experiments. Below, we shall study the maximal mean QFI of the GHZ state in these channels.

IV. MAXIMAL MEAN QFI UNDER DECOHERENCE

After a brief overview of the decoherence channels, now we study the maximal mean QFI of the GHZ state in these channels. The N-qubit GHZ state can be written in the form of a density matrix as

$$\rho_{rmGHZ} = |0\rangle\langle 0|^{\otimes N} + |0\rangle\langle 1|^{\otimes N} + |1\rangle\langle 0|^{\otimes N} + |1\rangle\langle 1|^{\otimes N}, \tag{17}$$

thus the density matrix $\rho_{\rm GHZ}$ has only four nonzero elements. Here, we assume that the decoherence channels act on the N qubits independently, and then the channel in Kraus representation reads

$$\begin{aligned} \mathcal{E}_{\rm total}(\rho_{\rm GHZ}) = {} & \mathcal{E}(|0\rangle\langle 0|)^{\otimes N} + \mathcal{E}(|0\rangle\langle 1|)^{\otimes N} \\ & + \mathcal{E}(|1\rangle\langle 0|)^{\otimes N} + \mathcal{E}(|1\rangle\langle 1|)^{\otimes N}, \end{aligned} \tag{18}$$

where $\mathcal{E}_{\rm total}$ represents the channel that acts on the total N-qubit system, and $\mathcal{E}$ represents the channel for a single qubit.

Below, we study the maximal mean QFI in the three channels separately. The explicit form of the density matrix $\rho = \mathcal{E}_{\rm total}(\rho_{\rm GHZ})$ is given for each channel. Then, the matrix $\mathbf{C}$ in Eq. (7) can be obtained by using the eigenvalues and eigenvectors of ρ.

Here, we first provide a main result of this article. For each channel, the matrix $\mathbf{C}$ is in a diagonal form as

$$\mathbf{C} = \begin{bmatrix} \mathbf{C}_{xx} & 0 & 0 \\ 0 & \mathbf{C}_{yy} & 0 \\ 0 & 0 & \mathbf{C}_{zz} \end{bmatrix}. \tag{19}$$

Moreover, we find $\mathbf{C}_{xx} = \mathbf{C}_{yy}$, therefore, we can denote $\mathbf{C}_\perp \equiv \mathbf{C}_{xx} = \mathbf{C}_{yy}$, and the maximal mean QFI becomes

$$\bar{F}_{\rm max} = \frac{1}{N}\max\{\mathbf{C}_\perp, \mathbf{C}_\parallel\} = \max\{\bar{F}_\perp, \bar{F}_\parallel\}. \tag{20}$$

The above result shows that, when the GHZ state undergoes the decoherence channels, it is most sensitive with respect to rotations in either the z direction or the x-y plane. The competition of the two terms leads to a sudden-change behavior.

A. Maximal mean QFI in ADC

For the ADC, by using Eq. (14), we find the GHZ state evolves to $\mathcal{E}_{\rm ADC}(\rho_{\rm GHZ}) = \varrho_1 \oplus \varrho_2$, where

$$\begin{aligned} \varrho_1 &= \frac{1}{2}\sum_{m=1}^{N-1} s^{N-m}p^m|0\rangle\langle 0|^{\otimes(N-m)}|1\rangle\langle 1|^{\otimes m}, \\ \varrho_2 &= \frac{1}{2}[s^N|0\rangle\langle 0|^{\otimes N} + s^{N/2}|0\rangle\langle 1|^{\otimes N} \\ &\quad + s^{N/2}|1\rangle\langle 0|^{\otimes N} + (1+p^N)|1\rangle\langle 1|^{\otimes N}]. \end{aligned} \tag{21}$$

By diagonalizing the above density matrices, we could obtain the matrix elements in Eq. (7), and then the QFI. The matrix ϱ_1 is already diagonal, and the eigenvalues of ϱ_2 are

$$\begin{aligned} \lambda_1 &= \tfrac{1}{2}(s^N + s^{N/2}\tan\theta), \\ \lambda_2 &= \tfrac{1}{2}[(1+p^N) - s^{N/2}\tan\theta], \end{aligned} \tag{22}$$

where $\theta = \frac{1}{2}\arctan\{2s^{N/2}/[s^N - (1+p^N)]\}$. The corresponding eigenvectors are

$$\begin{aligned} |\psi_1\rangle &= \cos\theta|0\rangle^{\otimes N} + \sin\theta|1\rangle^{\otimes N}, \\ |\psi_2\rangle &= \cos\theta|1\rangle^{\otimes N} - \sin\theta|0\rangle^{\otimes N}. \end{aligned} \tag{23}$$

By inserting the above results into Eq. (7), we calculate the matrix $\mathbf{C}$ straightforwardly and find that it is of the form as Eq. (19), with $\mathbf{C}_{xx} = \mathbf{C}_{yy}$. Since in the ADC the mean spin direction is along the z direction, we denote $\mathbf{C}_\perp = \mathbf{C}_{xx} = \mathbf{C}_{yy}$ and $\mathbf{C}_\parallel = \mathbf{C}_{zz}$, where the subscripts $\perp$ and $\parallel$ represent directions perpendicular to and parallel to the mean

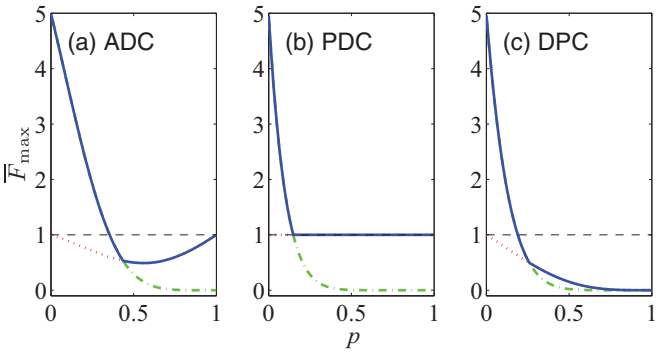

FIG. 1. (Color online) Maximal mean QFI $\bar{F}_{\max}$ (blue solid line) as a function of p is plotted for (a) amplitude-damping channel, (b) depolarizing channel, and (c) phase-damping channel. The initial state is a five-body GHZ state, and $\bar{F}_{\max} = N - 5$ at $p = 0$. The (red) dotted line denotes $\bar{F}_{\perp}$, and the (green) dash-dotted line denotes $\bar{F}_{\parallel}$. The horizontal dashed line denotes 1.

spin direction, respectively. We obtain

$$\begin{aligned}\mathbf{C}_{\perp} &= -\frac{N}{2}(p-s)^2[\,p^{N-1} - 1 + s^{N-1}] \\ &\quad + N\sum_{i=1}^{2}\cos^2\gamma\,\frac{\left(\lambda_i - \frac{1}{2}s\,p^{N-1}\right)^2}{\lambda_i + \frac{1}{2}s\,p^{N-1}} \\ &\quad + \sin^2\gamma\,\frac{\left(\lambda_i - \frac{1}{2}s^{N-1}p\right)^2}{\lambda_i + \frac{1}{2}s^{N-1}p}, \\ \mathbf{C}_{\parallel} &= \frac{2N^2 s^N}{1 + p^N + s^N}. \end{aligned} \tag{24}$$

Therefore, we have

$$\bar{F}_{\max} = \max\{\bar{F}_{\perp}, \bar{F}_{\parallel}\} = \frac{1}{N}\max\{\mathbf{C}_{\perp}, \mathbf{C}_{\parallel}\}. \tag{25}$$

The results show that the maximal mean QFI is determined by two quantities: (i) the mean QFI in the x-y plane denoted by $\bar{F}_{\perp}$; (ii) the mean QFI in the z direction denoted by $\bar{F}_{\parallel}$. According to the physical description of the QFI, $\bar{F}_{\perp}$ and $\bar{F}_{\parallel}$ denote the sensitivities of the state with respect to SU(2) rotations in the x-y plane and in the z direction, respectively.

The above results of $\bar{F}_{\max}$, $\bar{F}_{\perp}$, and $\bar{F}_{\parallel}$ are plotted in Fig. 1(a). There are two special points that are easy to analyze. One of them is at $p = 0$, when no decoherence occurs and the sensitivity of the GHZ state with respect to rotations along the z direction can achieve the Heisenberg limit $\bar{F}_{\max} = \bar{F}_{\parallel} = N$, however, the sensitivity of the system with respect to rotations in the x-y planes only achieve the shot-noise level $\bar{F}_{\perp} = 1$. The other point is at $p = 1$, where the state is fully populated in the ground state $|1\rangle$ due to the relaxation nature of the ADC (i.e., the state is a coherent spin state pointed to the $-z$ direction). Thus the sensitivity of the state with respect to rotations in the x-y plane achieves the shot-noise level (i.e., $\bar{F}_{\perp} = 1$). On the other hand, the state is invariant with respect to rotations along the z direction, thus $\bar{F}_{\parallel} = 0$.

When decoherence occurs ($p \neq 0$), we find that $\bar{F}_{\parallel}$ decays from N to 0 with the increase of p, while $\bar{F}_{\perp}$ decays from 1 at first and then increases to 1 at $p = 1$. Thus, there exist a sudden-change point p_s^{ADC} at which $\bar{F}_{\parallel} = \bar{F}_{\perp}$. The critical point is at $p = p_c^{\mathrm{ADC}}$, where $\bar{F}_{\max} = \bar{F}_{\parallel} = 1$, and when $p \geqslant p_c^{\mathrm{ADC}}$ the state cannot be used to overcome the shot-noise level estimation. The position of the critical point can be derived approximately as

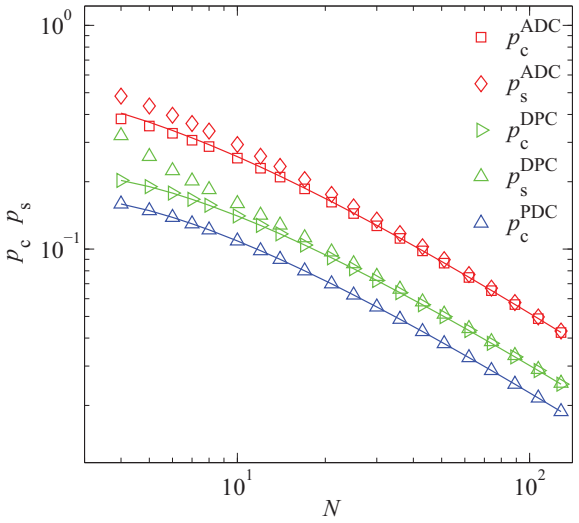

FIG. 2. (Color online) Critical points p_c and sudden change point p_s as functions of system size N are plotted in log-log axis. The solid lines are analytical results of p_c. For the large-N case, p_c and p_s are approximately equal, and the analytical results (solid line) fit well.

$$p_c^{\mathrm{ADC}} \simeq 1 - \left(\frac{1}{2N}\right)^{1/N}, \tag{26}$$

and this is shown in Fig. 2, with numerical results. For the large-N case, the sudden-changing point p_s^{ADC} is approximately equal to the critical point p_c^{ADC}, and the numerical results are shown in Fig. 2.

To compare with a concrete physical model that undergoes dissipation, we can replace the decoherence strength p with $1 - \exp(-\gamma_1 t/2)$, where γ_1 is the relaxation rate. Thus the critical point p_c^{ADC} corresponds to a critical time

$$t_c^{\mathrm{ADC}} \simeq \frac{2\ln 2N}{N\gamma_1}. \tag{27}$$

For times longer than t_c^{ADC}, the GHZ state is useless for entanglement-enhanced metrology.

B. Maximal mean QFI in PDC

The evolution under the PDC is easier to analyze. For the GHZ state, only the two nondiagonal terms decay, and the state becomes

$$\begin{aligned}\mathcal{E}_{\mathrm{PDC}}(\rho_{\mathrm{GHZ}}) &= \tfrac{1}{2}[|0\rangle\langle 0|^{\otimes N} + |1\rangle\langle 1|^{\otimes N}] \\ &\quad + \tfrac{1}{2}s^N[|0\rangle\langle 1|^{\otimes N} + |1\rangle\langle 0|^{\otimes N}], \end{aligned} \tag{28}$$

which can be diagonalized readily. The matrix elements of $\mathbf{C}$ is obtained as

$$\mathbf{C}_{\perp} = N, \quad \mathbf{C}_{\parallel} = N^2(1-p)^{2N}, \tag{29}$$

and thus

$$\bar{F}_{\max} = \max\{\bar{F}_{\perp}, \bar{F}_{\parallel}\} = \max\{1, N(1-p)^{2N}\}. \tag{30}$$

At $p = 1$, the states become a classical superposition of two coherent spin states that polarize to the z and $-z$ directions,

respectively, thus $\bar{F}_\perp = 1$ and $\bar{F}_\parallel = 0$, shown in Fig. 1(b). Therefore, with the increase of p, $\bar{F}_{\max}$ decays from N to 1, and the critical point

$$p_c^{\mathrm{PDC}} = 1 - \left(\frac{1}{N}\right)^{1/2N}, \tag{31}$$

which is also the sudden-changing point of $\bar{F}_{\max}$, which is plotted in Fig. 2.

In Ref. [30], a concrete phase-damping model is studied, where the damping rate γ_2 is associated with p as $p = 1 - \exp(-\gamma_2 t/2)$, therefore

$$\bar{F}_\parallel = N \exp(-N\gamma_2 t). \tag{32}$$

The decay rate of the coherence of the GHZ state is N times larger than a single qubit. After the critical time

$$t_c^{\mathrm{PDC}} = \frac{\ln N}{N\gamma_2}, \tag{33}$$

the GHZ state cannot be used to perform over shot-noise estimation. Furthermore, we obtain

$$\frac{t_c^{\mathrm{ADC}}}{t_c^{\mathrm{PDC}}} \simeq \frac{2T_1}{T_2}, \tag{34}$$

where $T_i = 1/\gamma_i$ are the typical damping times of dissipation and dephasing. This result can give us a criterion to determine which type of decoherence affects the QFI the most in experiments.

C. Maximal mean QFI in DPC

In the depolarizing channel, the state evolves to $\mathcal{E}_{\mathrm{DPC}}(\rho_{\mathrm{GHZ}}) = \tilde{\varrho}_1 \oplus \tilde{\varrho}_2$, where

$$\begin{aligned}
\tilde{\varrho}_1 &= \sum_{m=1}^{N-1} (\eta_m + \eta_{N-m}) |0\rangle\langle 0|^{\otimes(N-m)} |1\rangle\langle 1|^{\otimes m}, \\
\tilde{\varrho}_2 &= \frac{s^N}{2} (|0\rangle\langle 1|^{\otimes N} + |1\rangle\langle 0|^{\otimes N}) \\
&\quad + \frac{1}{2}[(1-\tilde{p})^N + \tilde{p}^N] |0\rangle\langle 0|^{\otimes N} \\
&\quad + \frac{1}{2}[(1-\tilde{p})^N + \tilde{p}^N] |1\rangle\langle 1|^{\otimes N},
\end{aligned} \tag{35}$$

where $\eta_m = \frac{1}{2}(1-\tilde{p})^m \tilde{p}^{N-m}$, $\tilde{p} = p/2$. The matrix $\tilde{\varrho}_1$ is already diagonal and the eigenvalues of $\tilde{\varrho}_2$ are

$$\begin{aligned}
\mu_1 &= \tfrac{1}{2}[(1-\tilde{p})^N + \tilde{p}^N + s^N], \\
\mu_2 &= \tfrac{1}{2}[(1-\tilde{p})^N + \tilde{p}^N - s^N],
\end{aligned} \tag{36}$$

with corresponding eigenvectors

$$\begin{aligned}
|\varphi_1\rangle &= \frac{1}{\sqrt{2}}(|0\rangle^{\otimes N} + |1\rangle^{\otimes N}), \\
|\varphi_2\rangle &= \frac{1}{\sqrt{2}}(|0\rangle^{\otimes N} - |1\rangle^{\otimes N}).
\end{aligned} \tag{37}$$

Inserting the above results into Eq. (7) we find

$$\begin{aligned}
\mathbf{C}_\perp &= \sum_{m=1}^{N-2} \frac{(p_m + p_{N-m} - p_{m+1} - p_{N-m-1})^2}{p_m + p_{N-m} + p_{m+1} + p_{N-m-1}} \\
&\quad \times (N-m)\binom{N}{m} + N \sum_{i=1}^{2} \frac{(\mu_i - p_1 - p_{N-1})^2}{\mu_i + p_1 + p_{N-1}}, \\
\mathbf{C}_\parallel &= \frac{N^2(1-p)^{2N}}{(1-\tilde{p})^N + \tilde{p}^N}.
\end{aligned} \tag{38}$$

The maximal mean QFI in this channel is plotted in Fig. 1(c). At $p = 1$, the state is completely depolarized, and is a fully mixed state, thus it is invariant under SU(2) rotations, and $\bar{F}_{\max} = 0$. The position of the critical point $\bar{F}_{\max} = 1$ can be derived approximately as

$$p_c^{\mathrm{DPC}} \simeq 1 - \frac{1}{4}\left(\frac{1}{N}\right)^{1/N} [1 + \sqrt{1 + 8N^{1/N}}]. \tag{39}$$

For the large-N case, the sudden-changing point p_s^{DPC} is approximately equal to the critical point p_c^{DPC}, and the numerical results are shown in Fig. 2. As discussed previously, if we replace $p = 1 - \exp(-\gamma_3 t/2)$, the critical time is obtained as

$$t_c^{\mathrm{DPC}} \simeq \frac{2\ln N}{N\gamma_3}. \tag{40}$$

In addition to the above results, note that the slopes of maximal mean QFI are different in the three channels. It decays most slowly in the ADC, and fastest in the PDC. This can be understood by using a Bloch sphere picture to imagine the decoherence channels. First, for $p < p_s$, we always have $\bar{F}_{\max} = \bar{F}_\parallel$, and the decay of $\bar{F}_\parallel$ is mainly caused by the shrink of the Bloch sphere in the x-y plane. As discussed in Sec. III, the radius of the Bloch sphere in the x-y plane is reduced by $\sqrt{1-p}$, $1-p$, and $1-2p$ for ADC, DPC, and PDC, respectively. Therefore, for a given p, the radius in the x-y plane reduces the most in the PDC, and thus in this channel the maximal mean QFI decays the fastest.

V. CONCLUSION

In this article, we studied the maximal mean QFI in three decoherence channels, the ADC, PDC, and DPC. Although sudden death is observed for both entanglement [46–48] and spin squeezing [49], the maximal mean QFI has a special feature: After the sudden-change point, in the ADC, the maximal mean QFI rises up with the increase of the decoherence strength. The initial state is the GHZ state, which can be used to improve the parameter estimation precision to the Heisenberg limit by measuring the parity operator. In the presence of decoherence, with the loss of entanglement, the sensitivity of the state with respect to SU(2) rotations becomes weaker. For sufficiently large decoherence strength p, the maximal mean QFI will decay to the shot-noise level, and we call these points the critical points p_c ($\bar{F}_{\max} = 1$). With the increase of p, for the ADC, the $\bar{F}_{\max}$ first decay below 1, then after sufficiently large p it increases to to 1; for the

PDC, the $\bar{F}_{\max}$ decays to 1 and remains in the shot-noise level; for the DPC, the $\bar{F}_{\max}$ decays to zero. We also observe the sudden-change points p_s, which are the crossing points of $\bar{F}_{\perp}$ and $\bar{F}_{\parallel}$. For the ADC and DPC, the critical points are derived approximately, and in the large-N limit, p_c and p_s are approximately equal, while for the PDC, exact results of the two points are obtained, and they are exactly equal. Moreover, our results are comparable with concrete physical models in a qualitative sense by replacing the decoherence strength p with a Markovian exponential decay function $1-\exp(-\gamma t/2)$. Based on this, we derived the critical time t_c ($\bar{F}_{\max}=1$) in terms of the decoherence time scale $T_i=1/\gamma_i$, which could help us to analyze the effects of different types of decoherence.

ACKNOWLEDGMENTS

Xiaoguang Wang acknowledges support from the NSFC with Grants No. 11025527, No. 10874151, and No. 10935010. Jian Ma acknowledges support from the Scholarship Grant for Excellent Doctoral Student granted by the Ministry of Education.

APPENDIX: MAXIMAL QFI

Below we show that the maximal QFI (9) is equal to the largest eigenvalue of matrix $\mathbf{C}$ (7). The maximal QFI is obtained by maximizing the QFI (6) over direction $\vec{n}$

$$F_{\max}=\max_{\vec{n}}(\vec{n}\,\mathbf{C}\,\vec{n}^{T}), \tag{A1}$$

where $\vec{n}=(n_1,n_2,n_3)$ is normalized [i.e., $(n_1)^2+(n_2)^2+(n_3)^3=1$]. Since the matrix $\mathbf{C}$ is symmetric, it can be diagonalized as

$$\mathbf{C}^{d}=O^{T}\,\mathbf{C}\,O=\mathrm{diag}\{\lambda_1,\lambda_2,\lambda_3\}, \tag{A2}$$

where the λ_i's are the eigenvalues of $\mathbf{C}$, and O is an orthogonal matrix (i.e., $O\,O^{T}$ and $O^{T}\,O$ are equal to an identity matrix). Therefore, the maximal QFI (A1) can be written as

$$\begin{aligned}F_{\max}&=\max_{\vec{n}}(\vec{n}\,O\,\mathbf{C}^{d}\,O^{T}\,\vec{n}^{T})\\&=\max_{\vec{n'}}(\vec{n'}\,\mathbf{C}^{d}\,\vec{n'}^{T}).\end{aligned} \tag{A3}$$

Note that, in the second line, we introduce a new direction

$$\vec{n'}=\vec{n}\,O, \tag{A4}$$

which is also normalized because O is orthogonal. Since $\mathbf{C}$ and O are independent of $\vec{n}$, the maximization in Eq. (A3) is performed over the new direction $\vec{n'}$. Now taking Eq. (A2) into Eq. (A3), we obtain

$$F_{\max}=\max_{\vec{n'}}[\lambda_1\,(n'_1)^2+\lambda_2\,(n'_2)^2+\lambda_3\,(n'_3)^2]. \tag{A5}$$

As $\vec{n'}$ is normalized $(n'_1)^2+(n'_2)^2+(n'_3)^2=1$, we have

$$F_{\max}=\max(\lambda_1,\lambda_2,\lambda_3), \tag{A6}$$

thus Eq. (9) is proved. In addition, if the maximal eigenvalue is λ_1, then $\vec{n'}=\vec{n}\,O=(1,0,0)$, and the original direction is

$$\vec{n}=(1,0,0)\,O^{T}. \tag{A7}$$

[1] C. W. Helstrom, *Quantum Detection and Estimation Theory* (Academic Press, New York, 1976).
[2] A. S. Holevo, *Probabilistic and Statistical Aspects of Quantum Theory* (North-Holland, Amsterdam, 1982).
[3] M. Hübner, Phys. Lett. A **163**, 239 (1992); **179**, 226 (1993).
[4] S. L. Braunstein and C. M. Caves, Phys. Rev. Lett. **72**, 3439 (1994).
[5] J. Preskill, *Lecture Notes for Physics 219: Quantum Information and Computation* (Caltech, Pasadena, CA, 1999).
[6] M. A. Nielsen and I. L. Chuang, *Quantum Computation and Quantum Information* (Cambridge University Press, Cambridge, England, 2000).
[7] M. Hayashi, *Quantum Information: An Introduction* (Springer-Verlag, Berlin, 2006).
[8] A. Uhlmann, Rep. Math. Phys. **9**, 273 (1976); **24**, 229 (1986).
[9] D. Bures, Trans. Am. Math. Soc. **135**, 199 (1969).
[10] W. K. Wootters, Phys. Rev. D **23**, 357 (1981).
[11] V. Giovannetti, S. Lloyd, and L. Maccone, Nature Photonics **5**, 222 (2011).
[12] J. J. Bollinger, W. M. Itano, D. J. Wineland, and D. J. Heinzen, Phys. Rev. A **54**, R4649 (1996).
[13] A. Peters, K. Y. Chung, and S. Chu, Nature (London) **400**, 849 (1999).
[14] R. Jozsa, D. S. Abrams, J. P. Dowling, and C. P. Williams, Phys. Rev. Lett. **85**, 2010 (2000).
[15] B. Yurke, S. L. McCall, and J. R. Klauder, Phys. Rev. A **33**, 4033 (1986).
[16] J. J. Bollinger, W. M. Itano, D. J. Wineland, and D. J. Heinzen, Phys. Rev. A **54**, R4649 (1996).
[17] J. P. Dowling, Phys. Rev. A **57**, 4736 (1998).
[18] P. Kok, S. L. Braunstein, and J. P. Dowling, J. Opt. B Quantum Semiclass. **6**, 5811 (2004).
[19] V. Giovannetti, S. Lloyd, and L. Maccone, Science **306**, 1330 (2004).
[20] V. Giovannetti, S. Lloyd, and L. Maccone, Phys. Rev. Lett. **96**, 010401 (2006).
[21] S. Boixo, S. T. Flammia, C. M. Caves, and J. M. Geremia, Phys. Rev. Lett. **98**, 090401 (2007).
[22] S. M. Roy and S. L. Braunstein, Phys. Rev. Lett. **100**, 220501 (2008).
[23] S. Boixo, A. Datta, M. J. Davis, S. T. Flammia, A. Shaji, and C. M. Caves, Phys. Rev. Lett. **101**, 040403 (2008).
[24] H. F. Hofmann, Phys. Rev. A **79**, 033822 (2009).
[25] M. Rosenkranz and D. Jaksch, Phys. Rev. A **79**, 022103 (2009).

[26] J. Estève, C. Gross, A. Weller, S. Giovanazzi, and M. K. Oberthaler, Nature (London) **455**, 1216 (2008).
[27] G. R. Jin and S. W. Kim, Phys. Rev. Lett. **99**, 170405 (2007).
[28] L. Pezzéand A. Smerzi, Phys. Rev. Lett. **102**, 100401 (2009).
[29] L. Hyllus, W. Laskowski, R. Krischek, C. Schwemmer, W. Wieczorek, H. Weinfurter, L. Pezzé, and A. Smerzi, e-print arXiv:1006.4366.
[30] S. F. Huelga, C. Macchiavello, T. Pellizzari, and A. K. Ekert, M. B. Plenio, and J. I. Cirac, Phys. Rev. Lett. **79**, 3865 (1997).
[31] D. Ulam-Orgikh and M. Kitagawa, Phys. Rev. A **64**, 052106 (2001).
[32] M. Sasaki, M. Ban, and S. M. Barnett, Phys. Rev. A **66**, 022308.
[33] A. Shaji and C. M. Caves, Phys. Rev. A **76**, 032111 (2007).
[34] A. Monras and M. G. A. Paris, Phys. Rev. Lett. **98**, 160401 (2007).
[35] Y. Li, Y. Castin, and A. Sinatra, Phys. Rev. Lett. **100**, 210401 (2008).
[36] R. Demkowicz-Dobrzański, U. Dorner, B. J. Smith, J. S. Lundeen, W. Wasilewski, K. Banaszek, and I. A. Walmsley, Phys. Rev. A **80**, 013825 (2009).
[37] T.-W. Lee, S. D. Huver, H. Lee, L. Kaplan, S. B. McCracken, C. Min, D. B. Uskov, C. F. Wildfeuer, G. Veronis, and J. P. Dowling, Phys. Rev. A **80**, 063803 (2009).
[38] U. Dorner, R. Demkowicz-Dobrzanski, B. J. Smith, J. S. Lundeen, W. Wasilewski, K. Banaszek, and I. A. Walmsley, Phys. Rev. Lett. **102**, 040403 (2009).
[39] Y. Watanabe, T. Sagawa, and M. Ueda, Phys. Rev. Lett. **104**, 020401 (2010).
[40] P. Hyllus, L. Pezzé, and A. Smerzi, Phys. Rev. Lett. **105**, 120501 (2010).
[41] J. Kołodyński, and R. Demkowicz-Dobrzański, Phys. Rev. A **82**, 053804 (2010).
[42] M. Kacprowicz, R. Demkowicz-Dobrzański, W. Wasilewski, K. Banaszek, and I. A. Walmsley, Nature Photonics **4**, 357 (2010).
[43] M. G. A. Genoni, S. Olivares, and M. G. Paris, Phys. Rev. Lett. **106**, 153603 (2011).
[44] A. W. Chin, S. F. Huelga, and M. B. Plenio, e-print arXiv:1103.1219.
[45] B. M. Escher, R. L. de MatosFilho, and L. Davidovich, Nature Physics **7**, 406 (2011).
[46] T. Yu and J. H. Eberly, Phys. Rev. Lett. **93**, 140404 (2004); Science **323**, 598 (2009).
[47] J. Laurat, K. S. Choi, H. Deng, C. W. Chou, and H. J. Kimble, Phys. Rev. Lett. **99**, 180504 (2007).
[48] M. P. Almeida, F. de Melo, M. Hor-Meyll, A. Salles, S. P. Walborn, P. H. Souto Ribeiro, and L. Davidovich, Science **316**, 579 (2007); A. Salles, F. de Melo, M. P. Almeida, M. Hor-Meyll, S. P. Walborn, P. H. Souto Ribeiro, and L. Davidovich, Phys. Rev. A **78**, 022322 (2008).
[49] X. Wang, A. Miranowicz, Y.-X. Liu, C. P. Sun, and F. Nori, Phys. Rev. A **81**, 022106 (2010).
[50] C. J. Myatt, B. E. King, Q. A. Turchette, C. A. Sackett, D. Kielpinski, W. M. Itano, C. Monroe, and D. J. Wineland, Nature (London) **403**, 269 (2000).
[51] Q. A. Turchette, C. J. Myatt, B. E. King, C. A. Sackett, D. Kielpinski, W. M. Itano, C. Monroe, and D. J. Wineland, Phys. Rev. A **62**, 053807 (2000).